Rigid Body Displacement Fields of an In-plane-deformable Curved Beam Based on Conventional Strain Definition

Moon Won-joo*, Kim Yong-woo and Min Oak-key*****

(Received November 20, 1997)

To improve the convergence and the accuracy of a finite element, the finite element has to describe not only displacement and stress distributions in a static analysis but also rigid body displacements. In this paper, we consider the in-plane-deformable curved beam element to understand the descriptive capability of rigid body displacements of a finite element. We derive the rigid body displacement fields of a single finite element under various essential boundary conditions when the nodal displacements are caused by the rigid body displacement. We also examine the rigid body displacement fields of a quadratic curved beam element by employing the reduced minimization theory.

Key Words: In-plane-deformable Curved Beam, Reduced Minimization, Rigid Body Displacement

1. Introduction

Many investigators have studied in-plane-deformable curved beam finite elements to improve the convergence and accuracy. Looking into their studies, many investigators have been interested in the cause and remedies of a stiffness locking phenomenon. As a result of these intensive studies, they have revealed that an inconsistent assumption on displacement functions produces spurious constraints when full integration is employed. The locking phenomenon in a static analysis is characterized by two typical numerical behaviors; one is a much smaller displacement than the exact one and the other is the violent undulate stress distributions.

Prathap and Babu (1986) explained how the full integration for shear and extensional strain energy leads to locking. Kamoulakos (1988) explained why reduced integration yields improved results by illustrating a simple example. He interpreted reduced integration as a process for degenerating a polynomial function to its least-squares fit by releasing a corresponding Legendre-like polynomial when a least-squares fit has to be achieved between two functions of different order. Min and Kim (1993, 1994, 1995) explained the role of a reduced integration from the viewpoint of minimization. They clarified the relationship amongst spurious constraints, optimal points, and integration order by using the reduced minimization theory.

To ensure convergence to the correct results, assumed displacement functions have to satisfy certain requirements (Zienkiewicz, 1989). One of them is a capability to describe rigid body displacements. This requirement is said as follows: the displacement function chosen should be such that it does not permit straining of an element to occur when the nodal displacements are caused by a rigid body displacement. Basically, the requirement needs only to be satisfied in the limit as the size of an element tends to zero. However, the imposition of the requirement on elements of a finite size leads to improved accuracy. Thus, based on this concept, we will examine the capability of a single element to describe rigid body

*Engineering Research Institute, Yonsei University
**Department of Mechanical Engineering, College of Engineering, Sunchon National University
***Department of Mechanical Design & Production Engineering, College of Engineering, Yonsei University

displacement fields when the nodal displacements are caused by a rigid body displacement.

In this paper, we will consider the same problem from a viewpoint of the reduced minimization theory to understand the descriptive capability of rigid body displacements of a finite element. For this goal, it is desirable to derive rigid body displacement fields of a single finite element under various essential boundary conditions when the nodal displacements are caused by a rigid body displacement. Thus, we will examine rigid body displacement fields of quadratic curved beam elements by employing the reduced minimization theory. The examination will clarify the role of reduced integration.

2. Strain Definition of an in-Plane-Deformable Curved Beam

The energy functional of an in-plane-deformable curved beam is given by:

$$U=\frac{1}{2}\int_s\{EA\varepsilon_t^2+kGA\gamma_b{}^2+EI\chi_b^2\}ds \tag{1}$$

where E is the Young's modulus, A is the cross sectional area, G is the shear modulus, I is the cross-sectional moments of inertia, k is the shear correction factor, ε_t is the extensional strain, γ_b is the shear strain, χ_b, is the bending strain, and s is the curvilinear coordinate running along the neutral axis of a curved beam.

The conventional strains (Prathap and Babu, 1986) are defined as

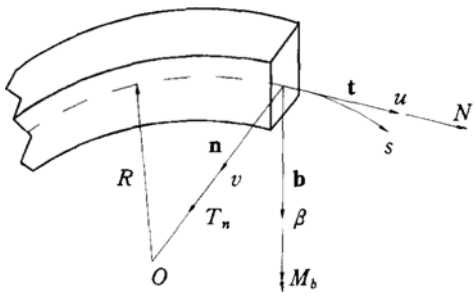

Fig. 1 Generalized displacements and unit vectors of an in-plane-deformable curved beam.

$$\begin{aligned}\varepsilon_t&=\frac{du}{ds}-\chi v\\ \gamma_b&=\frac{dv}{ds}-\beta\\ \chi_b&=\frac{d\beta}{ds}+\chi\frac{du}{ds}\end{aligned} \tag{2}$$

where u is a $\mathbf{t}$-directional displacement, v is a $\mathbf{n}$-directional deflection and β is quoted as a rotation of the cross section, as shown in Fig. 1.

3. Reduced Minimization Under Rigid Body Displacements

The functional of C^0-continuous beams (Min and Kim, 1994) can be written, in general, as:

$$U=U_U+U_C \tag{3}$$

where subscripts U and C denote the unconstrained energy and the constrained energy, respectively. These energies U_U and U_C can be composed of several strain energies and are expressed as:

$$U_U=\sum_{i=1}^{M}(\boldsymbol{U}_U)_i=\sum_{i=1}^{M}C_i\int_s(\varepsilon_i)^2ds \tag{4}$$

and

$$\boldsymbol{U}_C=\sum_{i=1}^{N}(U_C)_i=\sum_{i=1}^{N}D_i\int_s(\gamma_i)^2ds \tag{5}$$

where ε_i's $(i=1, 2, 3, \cdots, M)$ are unconstrained strains and γ_i's $(i=1, 2, 3, \cdots, N)$ are constrained strains; C_i's and D_i's are appropriate elastic constants; M is the number of unconstrained strain components and N is the number of constrained strain components.

In rigid body displacement fields, the minimization of the functional in Eq. (3) is equivalent to minimizing each strain energy since each strain energy should be zero:

$$\delta(C_i\int_s(\varepsilon_i)^2ds)=0,\ i=1, 2, 3, \cdots, M \tag{6}$$

$$\delta(D_i\int_s(\gamma_i)^2ds)=0,\ i=1, 2, 3, \cdots, N \tag{7}$$

3.1 Minimization of constrained energy under rigid body displacements

If we denote typical constrained strains as

$$\gamma = P(\xi) + \frac{dQ(\xi)}{ds} = P(\xi) + \frac{d\xi}{ds}\frac{dQ(\xi)}{d\xi} \tag{8}$$

where $P(\xi)$ and $Q(\xi)$ are typical displacements defined with respect to element coordinate $\xi(-1 \leq \xi \leq +1)$ and $d\xi/ds = const.$ under uniform isoparametric mapping. If the displacements P and Q are approximated by a polynomial of degree $(n-1)$, they are expressed as:

$$P(\xi) = \sum_{k=0}^{n-1} a_k \xi^k \tag{9}$$

$$Q(\xi) = \sum_{k=0}^{n-1} b_k \xi^k \tag{10}$$

where a_k's and b_k's are generalized displacement coordinates. By using Eqs. (9) and (10), the typical constrained strain component is expressed as:

$$\gamma = A^*_{n-1}\xi^{n-1} + \sum_{k=0}^{n-2} A_k \xi^k \tag{11}$$

where A_k's are matched coefficients contributed from all the field variables relevant to γ and A^*_{n-1} is unmatched coefficient that has coefficients only partially from the contributing field variables. They are expressed as

$$A^*_{n-1} = a_{n-1} \tag{12}$$

$$A_k = a_k + \frac{d\xi}{ds}(k+1)\, b_{k+1} \quad (k=0, 1, 2, \cdots, n-2) \tag{13}$$

By substituting the strain in Eq. (11) into a typical constrained strain in Eq. (7), we attempt to make;

$$\frac{\partial}{\partial a_k}\left(D\int_s \gamma^2\, ds\right) = 0, \; k=0, 1, 2, \cdots, n-1 \tag{14}$$

$$\frac{\partial}{\partial b_k}\left(D\int_s \gamma^2\, ds\right) = 0, \; k=0, 1, 2, \cdots, n-1 \tag{15}$$

where D is appropriate constant and we obtain

$$\int_s \gamma \xi^j\, ds = 0, \; j=0, 1, 2, \cdots, n-1 \tag{16}$$

$$\int_s \gamma \xi^j\, ds = 0, \; j=0, 1, 2, \cdots, n-2 \tag{17}$$

Equations (16) and (17) are equivalent to the minimization of the constrained energy, $(U_C)_i$, in Eq. (3) when displacements are approximated by n-noded interpolation.

The minimization of the constrained energy by Eq. (16) produces the constraints

$$A^*_{n-1} = 0 \tag{18}$$

$$A_k = 0 \; (k=0, 1, 2, \cdots, n-2) \tag{19}$$

The constraint in Eq. (18) is a spurious constraint that imposes an incompatible constraint on the assumed displacement fields (Prathap, 1985; Prathap and Babu, 1986). The constraints in Eq. (19) are true constraints. The minimization by Eq. (17) produces only the true constraints in Eq. (19). We call this kind of minimization that produces only true constraints 'reduced minimization' (Min and Kim, 1994; Kim and Min, 1993, 1995). The set of Eqs. (16) or (17) are called 'error-moment equations'.

In general cases, the reduced minimization by the error-moment equation can be restated as follows (Min and Kim, 1994):

Theorem 1

When the displacements are approximated by complete polynomials of degree $(n-1)$, the constrained strain is expressed as:

$$\gamma = A^*_{n-1}\xi^{n-1} + A_{n-2}\xi^{n-2} + A_{n-3}\xi^{n-3} + \cdots + A_1\xi + A_0$$

where A^*_{n-1} is the unmatched coefficient and A_k's $(k = n-2, n-3, \cdots, 0)$ are matched coefficients.

Let

$\mathbf{F} = \{F_k = \xi^{k-1} \; ; \; k=1, 2, 3, \cdots, n\}$

$\mathbf{R} = \{R_k = \xi^{k-1} \; ; \; k=1, 2, 3, \cdots, n-1\}$, and

$\mathbf{W} = \{W_k \; : \; k=1, 2, 3, \cdots, m\}$

The error-moment equations that minimize the constrained strain energy are given for

$$\int_{-1}^{+1} \gamma W_k d\xi = 0, \; k=1, 2, 3, \cdots, m \tag{20}$$

(1) If $W_k = F_k$(where $m=n$), the n error-moment equations produce one spurious constraint and $(n-1)$ independent true constraints. This is called full minimization.

(2) If $W_k = R_k$(where $m=n-1$), the $(n-1)$ error-moment equations produce $(n-1)$ independent true constraints. This is called reduced minimization.

Once a spurious constraint is produced in a constraining limit such as $KGA \gg EI$ and $EA \gg$

EI, the spurious constraint increases the unconstrained energy's stiffness that causes locking and very poor convergence (Prathap, 1985; Prathap and Babu, 1986). If reduced minimization is used for constrained energies, no spurious constraint is generated and thus no locking is caused.

3.2 Minimization of unconstrained energy under rigid body displacements

The reduced minimization of unconstrained energy under rigid body displacements can also be derived by the same manner demonstrated for constrained energy in the previous section. However the presence of an unmatched coefficient in a discretized unconstrained strain is immaterial because it does not lead to locking. Moreover, the bending strain of the in-plane-deformable curved beam under consideration, which is the unconstrained strain, does not have an unmatched coefficient. For example, consider the conventional bending strain in Eq. (2).

If we assume the displacement as follows:

$$\beta(\xi)=\sum_{k=0}^{n-1} c_k \xi^k \tag{21}$$

$$u(\xi)=\sum_{k=0}^{n-1} d_k \xi^k \tag{22}$$

then the discretized bending strain is expressed, under an uniform isoparametric mapping, as

$$\chi_b=\sum_{k=0}^{n-2} B_k \xi^k \tag{23}$$

where $B_k=(k+1)\frac{d\xi}{ds}(c_{k+1}+\chi d_{k+1})$, which are matched coefficients.

By substituting the strain in Eq. (23) into Eq. (6), we attempt to make;

$$\frac{\partial}{\partial c_k}\left(EI\int_s \chi_b^2\, ds\right)=0,\ k=0,\ 1,\ 2,\ \cdots,\ n-1 \tag{24}$$

$$\frac{\partial}{\partial d_k}\left(EI\int_s \chi_b^2\, ds\right)=0,\ k=0,\ 1,\ 2,\ \cdots,\ n-1 \tag{25}$$

and we obtain the error-moment equations:

$$\int_s \chi_b \xi^k\, ds=0,\ k=0,\ 1,\ 2,\ \cdots,\ n-2 \tag{26}$$

Equation (26) is equivalent to the minimization of the bending energy when β and u are approximated by n-noded interpolations.

The minimization of the bending energy by Eq. (25) produces the $(n-1)$ true constraints

$$B_k=0\ (k=0,\ 1,\ 2,\ \cdots,\ n-2) \tag{27}$$

It should be noted that the additional error-moment equation corresponding to $k=n-1$ in Eq. (27) does not introduce any additional constraints since the additional equations will be dependent ones on the set of error-moment equations in Eq. (26) (Min and Kim, 1994).

We can obtain the same results for the new bending strain energy. Based on the above discussions, the minimization of bending energy can be summarized in parallel with Theorem 1 as follows;

Theorem 2

When the relevant displacements of bending strain are approximated by complete polynomials of degree $(n-1)$, the bending strain is expressed as

$$\chi_b=B_{n-1}\xi^{n-1}+B_{n-2}\xi^{n-2}+B_{n-3}\xi^{n-3}+\cdots+B_1\xi+B_0$$

where the coefficients B_k's are matched coefficients.

Let

$\mathbf{F}=\{F_k=\xi^{k-1}\ ;\ k=1,\ 2,\ 3,\ \cdots,\ n\}$
$\mathbf{R}=\{R_k=\xi^{k-1}\ ;\ k=1,\ 2,\ 3,\ \cdots,\ n-1\}$, and
$\mathbf{W}=\{W_k\ ;\ k=1,\ 2,\ 3,\ \cdots,\ m\}$

The error-moment equations that minimize the unconstrained strain energy are given by

$$\int_{-1}^{+1} \chi_b W_k d\xi=0,\ k=1,\ 2,\ 3,\ \cdots,\ m \tag{28}$$

(1) If $W_k=R_k$ where $m=n$, (i. e. full minimization), the n error-moment equations produce $(n-1)$ true constraints.

(2) If $W_k=R_k$ where $m=n-1$, (i. e. reduced minimization), the $(n-1)$ error-moment equations produce the same $(n-1)$ independent true constraints as the full minimization produces.

3.3 Correspondence between minimization types and integration techniques

There exists a correspondence between minimization types and conventional integration techniques, as shown in Table 1. Uniformly full minimization (UFM) is defined as the minimiza-

Table 1 Correspondence between minimization types and integration schemes. F. M. and R. M. denote full minimization and reduced minimization, respectively and F. I. and R. I. denote full integration and reduced integration, respectively.

Energy type \ Type of minimization (Integration schemes)	UFM (UFI)	SRM (SRI)	URM (URI)
Unconstrained energy	F. M. (F. I.)	F. M. (F. I.)	R. M. (R. I.)
Constrained energy	F. M. (F. I.)	R. M. (R. I.)	R. M. (R. I.)

Table 2 Number of integration points for a quadratic in-plane deformable curved beam element.

Integration Scheme \ Number of Integration	Extensional Strain	Shear Strain	Bending Strain
UFI	3	3	3
URI	2	2	2
SRI	2	2	3

tion of each strain energy by the full minimization. Selective reduced minimization (SRM) minimizes the unconstrained energy by the full minimization and the constrained energy by the reduced minimization. Uniformly reduced minimization (URM) is the minimization of each strain energy by the reduced minimization. UFM, SRM and URM can be performed by using uniformly full integration (UFI), selective reduced integration (SRI), and uniformly reduced integration, respectively (Min and Kim, 1994).

For example, three kinds of minimization of the quadratic in-plane-deformable curved beam element can be performed using the corresponding integration schemes as shown in Table 2.

4. Theoretical Rigid Body Displacement Field of a Single Unconstrained Element

In the previous section, we explained the conventional strain definition and energy functional for curved beam analysis and suggested a reduced minimization theory under rigid body displacement. In this section, we will derive the theoretical rigid body displacement fields for the conventional strain definition using the reduced minimization theory.

If the displacements are approximated in natural coordinate $(-1\leq\xi\leq+1)$ by an isoparametric interpolation of degree two

$$\begin{aligned} u&=a_0+a_1\xi+a_2\xi^2\\ v&=b_0+b_1\xi+b_2\xi^2\\ \beta&=c_0+c_1\xi+c_2\xi^2 \end{aligned} \tag{29}$$

then we get the discretized strains in local coordinate as follows:

$$\begin{aligned} \varepsilon_t&=\frac{du}{ds}-\chi v\\ &=\frac{du}{d\xi}\frac{d\xi}{ds}-\chi v\\ &=\left(\frac{d\xi}{ds}a_1-\chi b_0\right)+\left(2\frac{d\xi}{ds}a_2-\chi b_1\right)\xi-\chi b_2\xi^2\\ &=(Ja_1-\chi b_0)+(2Ja_2-\chi b_1)\,\xi-\underline{\chi b_2}\xi^2 \end{aligned} \tag{30}$$

$$\begin{aligned} \gamma_b&=\frac{dv}{ds}-\beta\\ &=\frac{dv}{d\xi}\frac{a\xi}{ds}-\beta\\ &=\left(\frac{d\xi}{ds}b_1-c_0\right)+\left(2\frac{d\xi}{\xi s}b_2-c_1\right)\xi-c_2\xi^2\\ &=(Jb_1-c_0)+(2Jb_2-c_1)\,\xi-\underline{c_2}\xi^2 \end{aligned} \tag{31}$$

$$\begin{aligned} \chi_b&=\frac{d\beta}{ds}+\chi\frac{du}{ds}\\ &=\frac{d\beta}{d\xi}\frac{d\xi}{ds}+\chi\frac{du}{d\xi}\frac{d\xi}{ds}\\ &=\frac{d\xi}{ds}(c_1+\chi a_1)+2\frac{d\xi}{ds}(c_2+\chi a_2)\,\xi\\ &=J(c_1+\chi a_1)+2J(c_2+\chi a_2)\,\xi \end{aligned} \tag{32}$$

where J denotes Jacobian determinant $(J=d\xi/ds)$ which has a constant value under uniform isoparametric mapping and underlined terms

mean unmatched coefficients. If the full integration is employed, unmatched coefficients which is included in the extensional strain and the shear strain produce the spurious constraints.

For each energy mode, the error-moment equations are given as follows:
for an extensional strain energy

$$\int_{-1}^{+1} \varepsilon_t \, d\xi = 0 \tag{33}$$

$$\int_{-1}^{+1} \varepsilon_t \, \xi \, d\xi = 0 \tag{34}$$

$$\int_{-1}^{+1} \varepsilon_t \, \xi^2 \, d\xi = 0 \tag{35}$$

for a shear strain energy

$$\int_{-1}^{+1} \gamma_b \, d\xi = 0 \tag{36}$$

$$\int_{-1}^{+1} \gamma_b \, \xi \, d\xi = 0 \tag{37}$$

$$\int_{-1}^{+1} \gamma_b \, \xi^2 \, d\xi = 0 \tag{38}$$

for a bending strain energy

$$\int_{-1}^{+1} \chi_b \, d\xi = 0 \tag{39}$$

$$\int_{-1}^{+1} \chi_b \, \xi \, d\xi = 0 \tag{40}$$

$$\int_{-1}^{+1} \chi_b \, \xi^2 \, d\xi = 0 \tag{41}$$

● Uniformly full integration

The constraints produced for UFI are obtained by using the nine error-moment equations (Eqs. 33~41). The error-moment equations produce the constraints

$$a_1 = a_2 = b_0 = b_1 = b_2 = c_0 = c_1 = c_2 = 0 \tag{42}$$

by which we obtain a rigid body displacement field of a single unconstrained element

$$\begin{aligned} u &= a_0 \\ v &= 0 \\ \beta &= 0 \end{aligned} \tag{43}$$

and we also obtain the discretized strain field as follows

$$\begin{aligned} \varepsilon_t &= 0 \\ \gamma_b &= 0 \\ \chi_t &= 0 \end{aligned} \tag{44}$$

● Uniformly reduced integration and selective reduced integration

The constraints produced SRI can be obtained by using the seven error-moment equations (Eqs. 33, 34, 36, 37, 39, 40, 41) of SRM, and the constraints produced for URI can be obtained by using the six error-moment equations (Eqs. 33, 34, 36, 37, 39, 40). However, the same results are produced by Theorem 2.

The error-moment equations produce the constraints:

$$\begin{aligned} a_1 &= \frac{6J\chi}{6J^2+\chi^2} b_0, \quad & a_2 &= \frac{3\chi}{6J^2+\chi^2} c_0 \\ b_1 &= \frac{6J}{6J^2+\chi^2} c_0, \quad & b_2 &= -\frac{3\chi^2}{6J^2+\chi^2} b_0 \\ c_1 &= -\frac{6J\chi^2}{6J^2+\chi^2} b_0, \quad & c_2 &= -\frac{3\chi^2}{6J^2+\chi^2} c_0 \end{aligned} \tag{45}$$

by which we obtain discretized displacement fields such as:

$$\begin{aligned} u &= a_0 + \frac{6Jkb_0}{6J^2+\chi^2}\xi + \frac{3\chi c_0}{6J^2+\chi^2}\xi^2 \\ v &= b_0 + \frac{6Jc_0}{6J^2+\chi^2}\xi - \frac{3\chi^2 b_0}{6J^2+\chi^2}\xi^2 \\ \beta &= c_0 - \frac{6J\chi^2 b_0}{6J^2+\chi^2}\xi - \frac{3\chi^2 c_0}{6J^2+\chi^2}\xi^2 \end{aligned} \tag{46}$$

We also obtain the approximated strain field as follows:

$$\begin{aligned} \varepsilon_t &= \frac{\chi^3 b_0}{6J^2+\chi^2}(3\xi^2-1) \\ \gamma_b &= \frac{\chi^2 c_0}{6J^2+\chi^2}(3\xi^2-1) \\ \chi_b &= 0 \end{aligned} \tag{47}$$

3. Theoretical Rigid Body Displacement Field of a Single Element Under Various Essential Boundary Conditions

In the previous section, we derived the theoretical rigid body displacement fields for the conventional strain definition using the reduced minimization theory. In this section, to exemplify the theoretical rigid body displacement fields, we will derive theoretical rigid body displacement fields of a single element subjected to various essential boundary conditions, as shown in Fig. 2.The first three characters in the parenthesis represent the left-end boundary conditions and the last three characters represent the right-end boundary conditions.

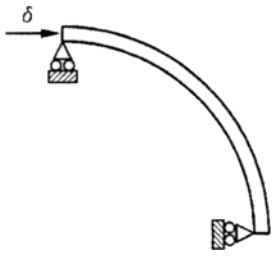

(a) Model- I (GZFFZF)

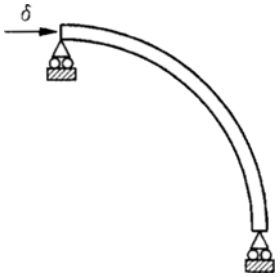

(b) Model- II (GZFZFF)

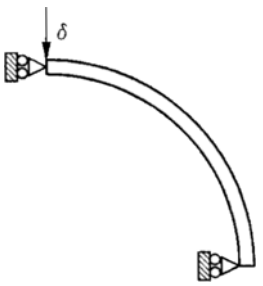

(c) Model- III (ZGFFZF)

Fig. 2 Numerical test models under rigid body displacements (G: given displacement, Z: zero displacement, F: free).

Example 1. Consider Model- I (GZFFZF) in Fig. 2 when the model is discretized by a single quadratic element. Model- I (GZFFZF) represents a rigid body rotational motion of the curved beam with respect to the center of curvature. We can obtain the theoretical rigid body displacement fields by imposing the rigid body displacement (δ) and boundary conditions.

The boundary conditions of Model- I (GZFFZF) are given by:

$$\begin{aligned} &u=\delta \text{ and } v=0 \quad at \quad \xi=-1 \\ &v=0 \qquad\qquad\quad at \quad \xi=+1 \end{aligned} \tag{48}$$

Applying the above boundary conditions to the rigid body displacement of a single unconstrained element, which was obtained in the previous section, we can obtain the displacement field of the constrained element.

If we use UFI, we can obtain the constraints by substituting the boundary conditions in Eq. (48) into Eq. (43). It follows that

$$\begin{aligned} &a_0=\delta \\ &b_0=c_0=0 \end{aligned} \tag{49}$$

By Eqs. (49) and (43), we obtain the theoretical rigid body displacement fields for the conventional strain definition as follows:

$$\begin{cases} u=\delta \\ v=0 \\ \beta=0 \end{cases} \tag{50}$$

If we use URI or SRI, Eq. (46) yields the following simultaneous equations by using the boundary conditions in Eq. (48):

$$\begin{cases} u\mid_{\xi=-1}=\delta=a_0-\dfrac{6J\chi}{6J^2+\chi^2}b_0+\dfrac{3\chi}{6J^2+\chi^2}c_0 \\ v\mid_{\xi=-1}=0=b_0-\dfrac{6J}{6J^2+\chi^2}c_0-\dfrac{3\chi^2}{6J^2+\chi^2}b_0 \\ v\mid_{\xi=+1}=0=b_0+\dfrac{6J}{6J^2+\chi^2}c_0-\dfrac{3\chi^2}{6J^2+\chi^2}b_0 \end{cases} \tag{51}$$

which produce the constraints:

$$\begin{aligned} &a_0=\delta \\ &b_0=c_0=0 \end{aligned} \tag{52}$$

By Eqs. (52) and (46), we obtain the theoretical rigid body displacement fields for the conventional strain definition as follows:

$$\begin{cases} u=\delta \\ v=0 \\ \beta=0 \end{cases} \tag{53}$$

From Eqs. (50) and (53), it can be seen that the theoretical rigid body displacement fields using UFI and those using URI or SRI show same results in the case of Model- I (GZFFZF).

Example 2. Consider Model- II (GZFZFF) in Fig. 2 when the model is discretized by a single quadratic element. Model- II (GZFZFF) represents a translational motion in the t-direction. The boundary conditions on Model- II (GZFZFF) are given by:

$$\begin{aligned} &u=\delta \text{ and } v=0 \quad at\ \xi=-1 \\ &u=0 \qquad\qquad\ at\ \xi=+1 \end{aligned} \tag{54}$$

Applying the above boundary conditions to the rigid body displacement of a single unconstrained element, we can obtain the displacement field of the constrained element.

If we use UFI, the rigid body displacement fields(Eq. 43) have only one unknown(a_0). However, rigid body displacement fields that satisfy the boundary conditions at the same time do not exist, as the number of boundary conditions is 3.This implies that the rigid body displacement of Model-II (GZFZFF) by the reduced minimization theory can not be described by a single quadratic element when UFI is used. On the contrary, if we use URI or SRI, the rigid body displacement fields(Eq. 46) have three unknowns(a_0, b_0, c_0), which are compatable to the number of boundary conditions.

If we use URI and SRI, Eq. (46) yields the following simultaneous equations by using the boundary conditions in Eq. (54).

$$\begin{cases} u \mid_{\xi=-1}=\delta=a_0-\dfrac{6J\chi}{6J^2+\chi^2}b_0+\dfrac{3\chi}{6J^2+\chi^2}c_0 \\ u \mid_{\xi=+1}=0=a_0+\dfrac{6J\chi}{6J^2+\chi^2}b_0+\dfrac{3\chi}{6J^2+\chi^2}c_0 \\ v \mid_{\xi=-1}=0=b_0-\dfrac{6J}{6J^2+\chi^2}c_0-\dfrac{3\chi^2}{6J^2+\chi^2}b_0 \end{cases} \tag{55}$$

which produce the constraints:

$$\begin{aligned} a_0&=\frac{9J^2-\chi^2}{12J^2} \\ b_0&=-\frac{6J^2+\chi^2}{12J\chi} \\ c_0&=-\frac{(6J^2+\chi^2)(3J^2-\chi^2)}{36J^2\chi}\delta \end{aligned} \tag{56}$$

By Eqs. (56) and (46), we obtain the theoretical rigid body displacement fields for the conventional strain definition as follows:

$$\begin{aligned} u&=\left[\frac{9J^2-\chi^2}{12J^2}-\frac{1}{2}\xi-\frac{3J^2-\chi^2}{12J^2}\xi^2\right]\delta \\ v&=\left[-\frac{6J^2+\chi^2}{12J\chi}-\frac{3J^2-\chi^2}{6J\chi}\xi+\frac{\chi}{4J}\xi^2\right]\delta \\ \beta&=\left[-\frac{(6J^2+\chi^2)(3J^2-\chi^2)}{36J^2\chi}+\frac{\chi}{2}s\right. \\ &\quad\left.+\frac{\chi(3J^2-\chi^2)}{12J^2}\xi^2\right]\delta \end{aligned} \tag{57}$$

Example 3. Consider Model-III (ZGFFZF) in Fig. 2 when the model is discretized by a single quadratic element. Model-III (ZGFFZF) represents a translational motion in the n-direction. The boundary conditions of Model-III (ZGFFZF) are given by:

$$\begin{aligned} &u=0 \text{ and } v=\delta \quad at\ \xi=-1 \\ &u=0 \qquad\qquad\ at\ \xi=+1 \end{aligned} \tag{58}$$

Applying the above boundary conditions to the rigid body displacement of a single unconstrained element, we can obtain the displacement field of the constrained element.

For the same reason as in Example 2, the rigid body displacement of Model-III (ZGFFZF) by the reduced minimization theory can not be described by a single quadratic element when UFI is used.

If we use URI and SRI, Eq. (46) yields the following simultaneous equations using the boundary conditions in Eq. (58):

$$\begin{cases} u \mid_{\xi=-1}=0=a_0-\dfrac{6J\chi}{6J^2+\chi^2}b_0+\dfrac{3\chi}{6J^2+\chi^2}c_0 \\ v \mid_{\xi=-1}=\delta=b_0-\dfrac{6J}{6J^2+\chi^2}c_0-\dfrac{3\chi^2}{6J^2+\chi^2}b_0 \\ v \mid_{\xi=+1}=0=b_0+\dfrac{6J}{6J^2+\chi^2}c_0-\dfrac{3\chi^2}{6J^2+\chi^2}b_0 \end{cases} \tag{59}$$

which produce the constraints:

$$\begin{aligned} a_0&=\frac{\chi(9J^2-\chi^2)}{4J(3J^2-\chi^2)}\delta \\ b_0&=-\frac{6J^2+\chi^2}{4J(3J^2-\chi^2)}\delta \\ c_0&=-\frac{6J^2+\chi^2}{12J}\delta \end{aligned} \tag{60}$$

By Eqs. (60) and (46), we obtain the theoretical rigid body displacement fields for the conventional strain definition as follows:

$$\begin{aligned} u&=\frac{\chi}{4J(3J^2-\chi^2)}[(9J^2-\chi^2)+6J^2\xi \\ &\quad-(3J^2-\chi^2)\xi^2]\delta \\ v&=\frac{1}{4J(3J^2-\chi^2)}[(6J^2+\chi^2)-2(3J^2-\chi^2)\xi \\ &\quad-3\chi^2\xi^2]\delta \\ \beta&=\left[-\frac{6J^2+\chi^2}{12J^2}-\frac{3J\chi^2}{2(3J^2-\chi^2)}\xi+\frac{\chi^2}{4J}\xi^2\right]\delta \end{aligned} \tag{61}$$

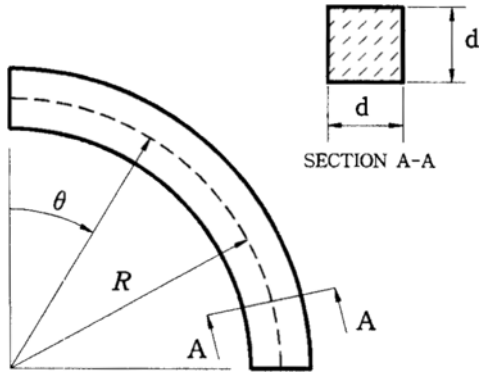

Fig. 3 Geometry of an in-plane-deformable curved beam.

Table 3 Exact solutions of three test models under rigid body displacements

MODEL	Exact Solutions
MODEL-I (GZFFZF)	$u=\delta$ $v=0$ $\beta=0$
MODEL-II (GZFZFF)	$u=\delta\cos\theta$ $v=-\delta\sin\theta$ $\beta=-\frac{\delta}{R}\cos\theta$
MODEL-III (ZGFFZF)	$u=\delta\sin\theta$ $v=\delta\cos\theta$ $\beta=-\frac{\delta}{R}\sin\theta$

6. Numerical Test

To prove the validity of theoretical predictions by the reduced minimization theory, we perform numerical tests when considering the capability of a single quadratic in-plane-deformable curved beam element to describe rigid body displacements. To do this, the theoretical rigid body displacements obtained by the present theory are compared with exact ones and finite element solutions. The test models used are shown in Fig. 3, of which the opening angle is $\pi/2$ with the square cross section. The radius of the curvature is 5 m, width of cross section is 0.1 m, and the imposed rigid body displacement (δ) is 0.1 m. The material properties of a curved beam are as follows:

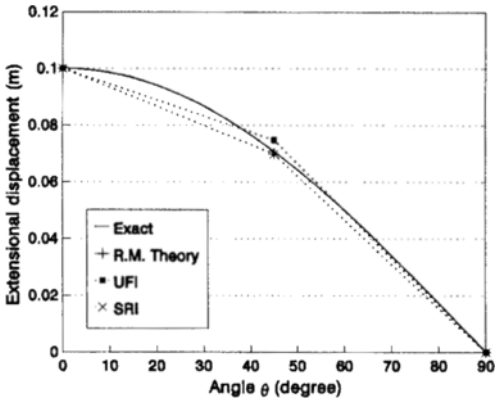

(a) Model-Ⅱ (GZFZFF)

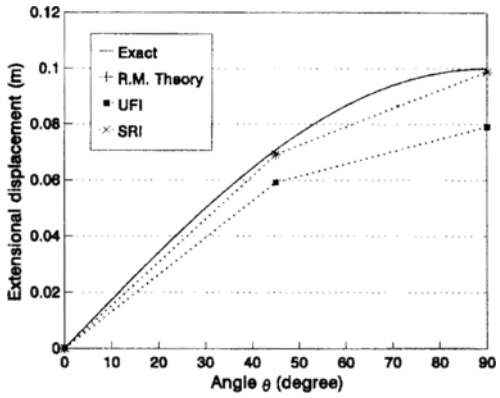

(b) Model-Ⅲ (ZGFFZF)

Fig. 4 Distribution of extensional displacement (u) using a single element.

Young's modulus : $E=2.07\times10^{11}\text{N/m}^2$

Shear modulus : $G=\frac{E}{2(1+\nu)}=8.023\times10^{10}\text{N/m}^2$

Poisson's ratio : $\nu=0.3$

Shear correction factor : $k=\frac{5}{6}$

To judge the accuracy of theoretical predictions, we derive the exact solutions of rigid body displacement fields of the test models using a transformation matrix. The exact rigid body displacements are shown in Table 3 and 1/R is equal to the constant curvature(χ) of the test models.

To examine the capability to describe rigid body displacements in relation to the integration schemes, we perform numerical tests for the three test models shown in Fig. 2 by using UFI, SRI

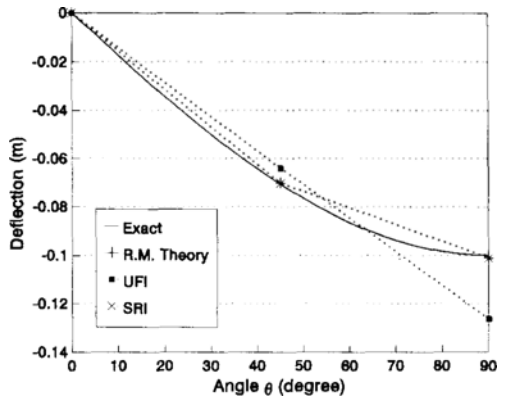

(a) Model-Ⅱ(GZFZFF)

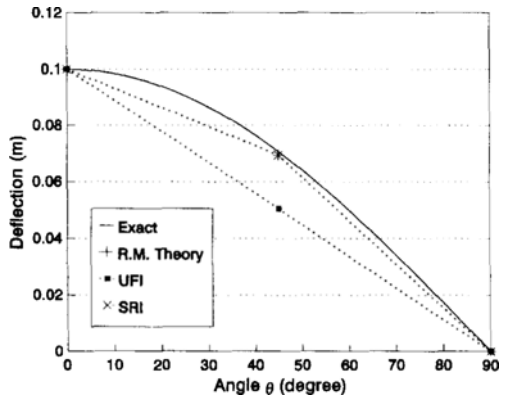

(b) Model-Ⅲ(ZGZFZF)

Fig. 5 Distribution of deflection (v) using a single element.

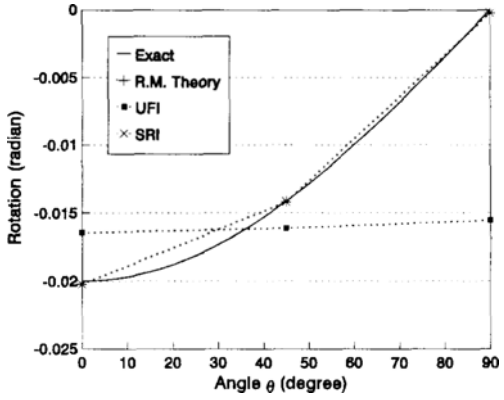

(a) Model-Ⅱ(GZFZFF)

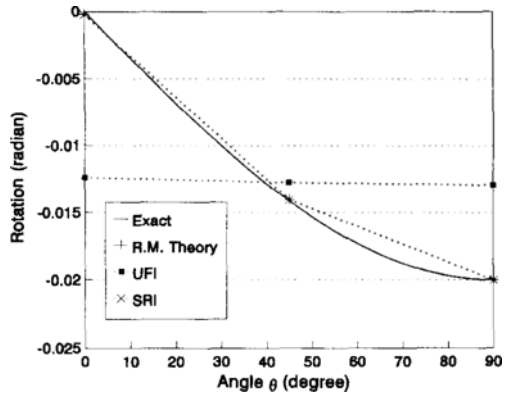

(b) Model-Ⅲ(ZGZFZF)

Fig. 6 Distribution of rotation (β) using a single element.

Table 4 Distribution of displacements of Model-Ⅰ(GZFFZF) discretized by a single element.

Displacement		Angle (Degree)	Exact	Present Theory	Numerical Solution	
					UFI	SRI
Conventional Strain Definition	u	0	0.1	0.1	1.0000E−01	1.0000E−01
		45	0.1	0.1	1.0000E−01	1.0000E−01
		90	0.1	0.1	1.0000E 01	1.0000E−01
	v	0	0.0	0.0	0.0000E+00	0.0000E+00
		45	0.0	0.0	2.7756E−17	−5.1023E−15
		90	0.0	0.0	0.0000E+00	0.0000E+00
	β	0	0.0	0.0	1.4610E−17	−2.5507E−15
		45	0.0	0.0	0.0000E+00	−1.7347E−17
		90	0.0	0.0	−1.2006E−17	2.6294E−15

and URI. The results are plotted in Figs. 4~6, where we don't do not present the finite element solutions obtained by URI since they are equal to the solutions obtained by SRI. We list the results

of Model-Ⅰ (GZFFZF) in Table 4 because they agree with the theoretical rigid body displacement fields by the reduced minimization theory. The exact solutions to each model are given in Table 3, and the present solutions by reduced minimization theory for each model are given in the previous section. In Figs. 4~6, the solid line represents the exact solution, the symbol '+' represents the reduced minimization's rigid body displacements which are derived in examples, i. e. Eqs. (57) and (61), the symbol '■' represents the numerical solution obtained by UFI, and the symbol '×' represents the numerical solution obtained by SRI. The symbols '+' and '×' are overplotted. Looking at the results in Figs. 4~6 and Table 4, we see the following facts:

1. The theoretical rigid body displacements of Model-Ⅰ (GZFFZF) agree with both the exact ones and finite element solutions, irrespective of the integration schemes used.
2. The finite element solutions of Model-Ⅱ (GZFZFF) and Model-Ⅲ (ZGFFZF), which are obtained using URI and SRI, agree with the theoretical ones obtained by the reduced minimization theory and are close to the exact ones.
3. The finite element solutions of Model-Ⅱ (GZFZFF) and Model-Ⅲ (ZGFFZF), which are obtained by using UFI, deviate from the exact ones.

From the above tests, we see that the finite element employing URI or SRI has a superior capability in describing the rigid body displacements to the element employing UFI.

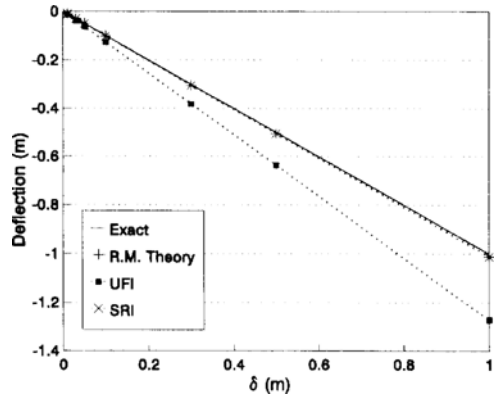

(a) Deflection(v) of Model-Ⅱ (GZFZFF)

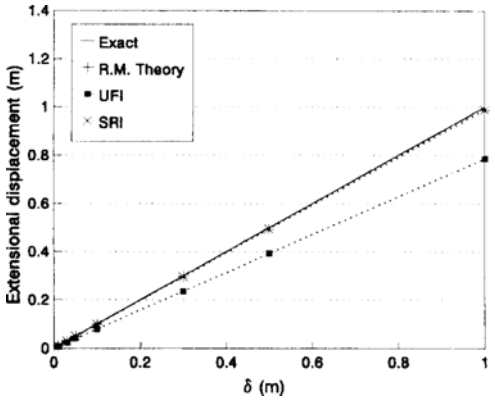

(c) Rotation(β) of Model-Ⅱ (GZFZFF)

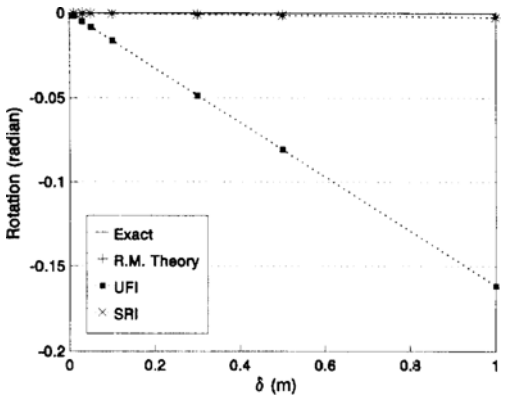

(b) Extensional Displacemcnt(u) of Model-Ⅲ (ZGZFZF)

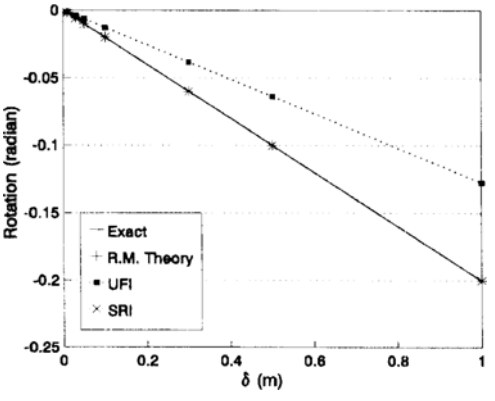

(d) Rotation(β) of Model-Ⅲ (ZGZFZF)

Fig. 7 Distribution of displacements at $\theta=\pi/2$ with respect to the rigid body displacement (δ) which is using a single element.

We perform another numerical test for Model-II (GZFZFF) and Model-III (ZGFFZF) to examine the displacement distributions in terms of the magnitude of imposed rigid body displacements (δ). In Fig. 7, we present the numerical results at $\theta=\pi/2$ for displacements except constrained displacements by boundary conditions. Figure 7 depicts the deflection of Model-II (GZFZFF), the extensional displacement of Model-III (ZGFFZF), and the rotation of Model-II (GZFZFF) and Model-III (ZGFFZF). In this numerical test, we employ the UFI and SRI. The magnitude of Fig. 7 shows that the SRI produces results very close to the exact ones, independent of the imposed rigid body displacement (δ). On the other hand, the UFI shows that the absolute error tends to increase as the imposed rigid body displacement (δ) increases.

From the above numerical results, we see that the URI or SRI can describe the rigid body displacements correctly, independent of the magnitude of an imposed rigid body displacement (δ). We can also evaluate the descriptive capability of rigid body displacements of a finite element without numerical tests.

7. Conclusion

To evaluate the descriptive capability of rigid body displacements of a finite element, we have derived the theoretical rigid body displacement fields of a single in-plane-deformable curved beam element based on the conventional strain definition under certain boundary conditions. To do this, we have suggested a theoretical method, which is called "reduced minimization under rigid body displacements." To compare the results obtained by using the theoretical method with numerical ones, various numerical tests for three models with different boundary conditions are carried out. The theoretical rigid body displacement fields by SRI can be obtained for all models using the reduced minimization theory and distributions of displacement agree with the numerical results. However, those by UFI cannot be obtained except for a certain model. The proposed method can be used to evaluate the descriptive capability of rigid body displacements of a finite element without numerical tests.

Acknowledgements

This study is supported by Korea Minister of Education through Research Fund (ME96-C-12), 1996.

References

Babu C. R. and Prathap G., 1986, "A linear Thick Curved Beam Element," *Int. J. Numer. Meth. Engng.*, Vol. 23, pp. 1313~1328

Kamoulakos A., 1988, "Understanding and Improving the Reduced Integration of Mindlin Shell Element," *Int. J. Numer. Meth. Engng.*, Vol. 26, pp. 2009~2029

Kim Yong-woo and Min Oak-key, 1993, "Theoretical Review on the Spurious Modes in Plane Stress/Strain Isoparametric Meshes," *Computers & Structures*, Vol. 49, pp. 1069~1082

Kim Yong-woo and Min Oak-key, 1995, "Reduced Minimization In Lagrangian Mindlin Plate Element with Arbitrary Orientation Under Uniform Isoparametric Mapping," *Int. J. Numer. Meth. Engng.*, Vol. 38, pp. 2101~2114

Kim Yong-woo and Min Oak-key, 1993, "A Performance Consideration on C^1-Continuous Thin Beam Element," *KSME Journal*, Vol. 7, pp. 303~311

Min Oak-key and Kim Yong-woo, 1994, "Reduced Minimization Theory in Beam Elements," *Int. J. Numer. Meth. Engng.*, Vol. 37, pp. 2125~2145

Prathap G., 1985, "The Curved Beam/Deep Arch/Finite Ring Element Revisited," *Int. J. Numer. Meth. Engng.*, Vol. 21, pp. 389~407

Prathap G. and Babu C. R., 1986, "An Isoparametric Quadratic Thick Curved Beam Element," *Int. J. Numer. Meth. Engng.*, Vol. 23, pp. 1583~1600

Stolarski H. and Belytschko T., 1981, "Membrane Locking and Reduced Integration for Curved Beam Elements," *Trans. of ASME, J. Appl. Mech.*, Vol. 49, pp. 172~176

Zienkiewicz O. C. and Taylor R. L., 1989, *The Finite Element Method* Vol. 1, 4th edn., McGraw-Hill